Phosphorous acid Functionalized Graphene oxide By Microwave and Evaluation as Anti-Corrosion inhibitor for carbon steel alloy Type C1025 in HCl Solution

***Ali A.Naser** ***Hadi Z Al-Sawaad** ***Alaa S.Al-Mubarak**

*ministry of education, Mayssan's directorate of education

**University of Basrah, College of Science, Department of Chemistry

Email: hadiziara@yahoo.com ***mobile: +9647801131734***

Correspond author: Email: aabra0595@gmail.com ***mobile: +647710498865***

الخلاصة

تمت دراسة كفاءة التثبيط لسبيكة الصلب الكاربوني من نوع C1025 في تركيز 0.1 مولاري من حامض الهيدروكلوريك عند درجة حرارة 298 كلفن بواسطة استعمال كل من أوكسيد الكرافين(GO) ومشتق من أوكسيد الكرافين بعد تطعيمه مع حامض الفسفوروز (GOE) . المركبات المحضرة شخصت بواسطة تقنيات عدة منها تقنية الأشعه تحت الحمراء(FT-IR)، والأشعه السينيه(XRD)، ومطيافية رامان (Raman shift)ومطيافية طاقة تشتت الأشعه السينيه(EDX) والمجهر الكتروني الماسح(FESEM) ، درست المركبات المحضرة باستخدام تقنيتين كهروكيميائيتين وهما طريقة مخطط تافل للاستقطاب (Tafel plot) ومطيافية قياس المعاوقه الكهروكيميائية EIS). حيث أوجدت النتائج بان عملية التثبيط للمركبات GOE,GO تحدث على سطح المعدن أو السبيكة . النتائج العملية الناتجة من مخطط تافل تشير بأن كفاءة التثبيط عند درجة حرارة 298 كلفن للمركبات المحضرة عند التركيز الاعظم كالآتي: (77.4% GO), GOE(86.8%) عند التركيز الاعظم ppm (70, 100) على التوالي .بينما تقنية مطيافية الامبدنس تستخدم لمناقشة ميانيكية التثبيط .

Abstract

Inhibition efficiency of carbon steel alloy type C1025 in 0.1 M HCl at 298 K by Graphene oxide (GO) and phosphorous acid Functionalized Graphene oxide (GOE) were synthesized and characterized by XRD, FT-IR, FESEM, Raman shift and EDX techniques afterward studied by two techniques Tafel plots and Impedance spectroscopy (EIS). The results reveals that inhibition take place during adsorption of GO and GOE on metal surface. Tafel plots reveals that optimal concentration of GO is 100 ppm with inhibition efficiency about 77.4 %, while GOE has 86.8 % at 70 ppm. EIS technique was used to discuss mechanism of inhibition.

Keywords: Graphene oxide, phosphorous acid, microwave, impedance. Tafel plot

1. Introduction

Corrosion is deterioration phenomenon of alloys and metals because interaction with environment, this is mean that the atoms leave alloy or metal to product compounds for these alloys in presence of gases and water**[1]**. Corrosion causes economic losses lead to total change of structure and equipment and also Corrosion is serious problem in the industry**[2, 3]**. To reduce corrosion that take place on carbon steel alloy surface are using compounds is called inhibitors which work adsorbing on alloy surface by generation film. Corrosion inhibitors classified into organic and inorganic types according to their chemical structures**[4]**.

Inhibitors are adsorbed on the metal surface either by physisorption or Chemisorption adsorption; organic inhibitors have heteroatoms groups such as O, N, S and P, both of types of adsorption take place because presence of heteroatoms groups for organic inhibitors **[5, 6]**.

Thus, graphene oxide and functionalized GOE have excellent corrosion inhibitors in acid solution due to graphene oxide (GO) has functional groups for various oxygen like carboxyl , carbonyl , hydroxyl and epoxide**[7-10]**.

The objective of work was functionalized graphene oxide with phosphorous acid and evaluates of them as corrosion inhibitor or prevents corrosion in acid solution (0.1 M HCl) for carbon steel alloy (C1025). This present study involves use of potentiodynamic polarization (Tafel plot) and electrochemical impedance spectroscopy (EIS).

2. Experimental

2.1. Materials

The carbon steel alloy which used in the present study was purchased from local the markets in Basrah city. The chemical compositions of carbon steel alloy C1025 were examined by metallurgical methods at the department of metallurgy in the college of Engineering; University of Basrah and the results are shown in Table 1.

Table1: carbon steel alloy composition (C1025).

Alloy	**Composition % w/w**								
Carbon steel (C1025)	C	S	P	Mn	Si	Cr	Ni	other	Fe
	0.27	0.002	0.003	0.69	0.2	0.029	0.008	0.3129	Balance

While the materials that used in this work were different material for different companies include : graphite powder, Aluminum chloride, Ammonium hydroxide ,Hydrogen peroxide ,Sodium nitrate, ,Sulphuric acid ,Hydrochloric acid ,Potassium permanganate, Ethanol ,N,N-Dimethyl formamide (DMF). Trietylamine (TEA), sodium hydroxide, bromine and phosphorous acid.

2.2. Synthesis of GO

Graphene oxide was prepared by using modified Hummer's method, in round bottom flask (RBF), 1 g of graphite powder, 23 mL of H_2SO_4 and 0.5 g sodium nitrate ($NaNO_2$) were mixed together under stirring for 30 min in ice bath. Then 3 g of KMnO4 added very slowly to the solution suspension for 3 h. after end amount of hydrogen peroxide (H_2O_2) was adding into the above mixture at reaction ceased. The obtained mixture was drying and exfoliation respectively by sonication for get GO solid and was repeatedly many times wash with 5% HCl and DI H_2O, Then the product was dried in furnace at (70-80°C) for 4 h to give GO**[11-13]**.

2.3. Synthesis of GOE

Firstly, graphene oxide was functionalized by amine group where, 0.5g of GO and 80 mL of $SOCl_2$ were mixed together under ultrasonic (Sonication (TF-1000)-China),for 2 h afterward the suspension was refluxed in 10 mL of DMF at 70°C for 24 h. Then suspension solution was filtered and washed for several times with DMF and deionized water and dried in air to overnight .The precipitated was mixed with 10mL of DMF , 14 mL (10 mmol) of trietylamine (TEA) and 5.49 mL of Ammonium hydroxide (NH_4OH)) in 100 mL dried beaker at ice bath (0 °C) for 1 h. Then the mixture was filtered by using vacuum filtration and washed with ammonia solution for many times, to get the product as black powder (amide-GO). The black powder was mixed with both of 50 mL of water ,5.76g of sodium hydroxide(NaOH) and 1.4 mL of bromine (Br_2) by Hoffman rearrangement ,where the mixture were stirred for 15 min at (0°C) ,afterward the mixture was stirred with temperature from (85-90)°C for 4 h**,** the reaction mixture filtered and washed with deionized water for several times and also dried in overnight, the product is black powder,(amine-GO)**[14]**. Secondly the product was functionalized by phosphorous acid by microwave 0.5 g of amine-GO are mixed with 0.82 g (10 mmole) of phosphorous acid were dispersed in 30 mL DMF by ultrasonic (Sonication (TF-1000)- China), for 30 min . Then 0.5g of $AlCl_3$ was added to the reaction mixture then again was sonicated for 30 min, the the above mixture put in microwave for 10 min at 20% (140 W).The final product was filtered and washed for several times with ethanol and deionized water and dried in air to overnight. The product is black powder, the general reaction as shown in the scheme2**[15]**.

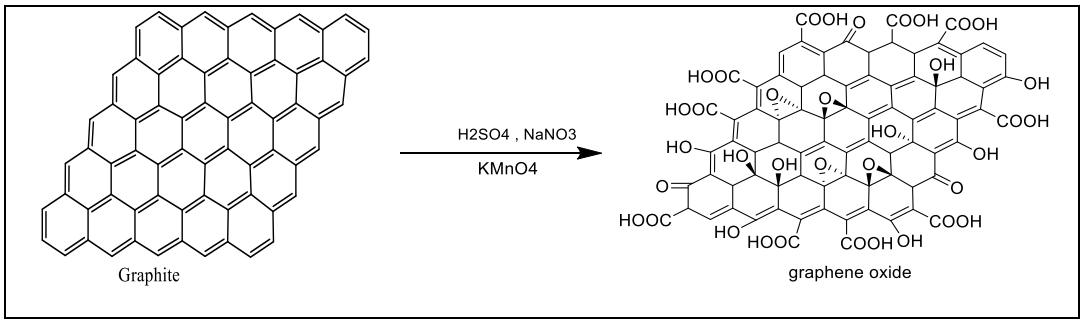

Scheme1: The chemical synthesis of GO compound.

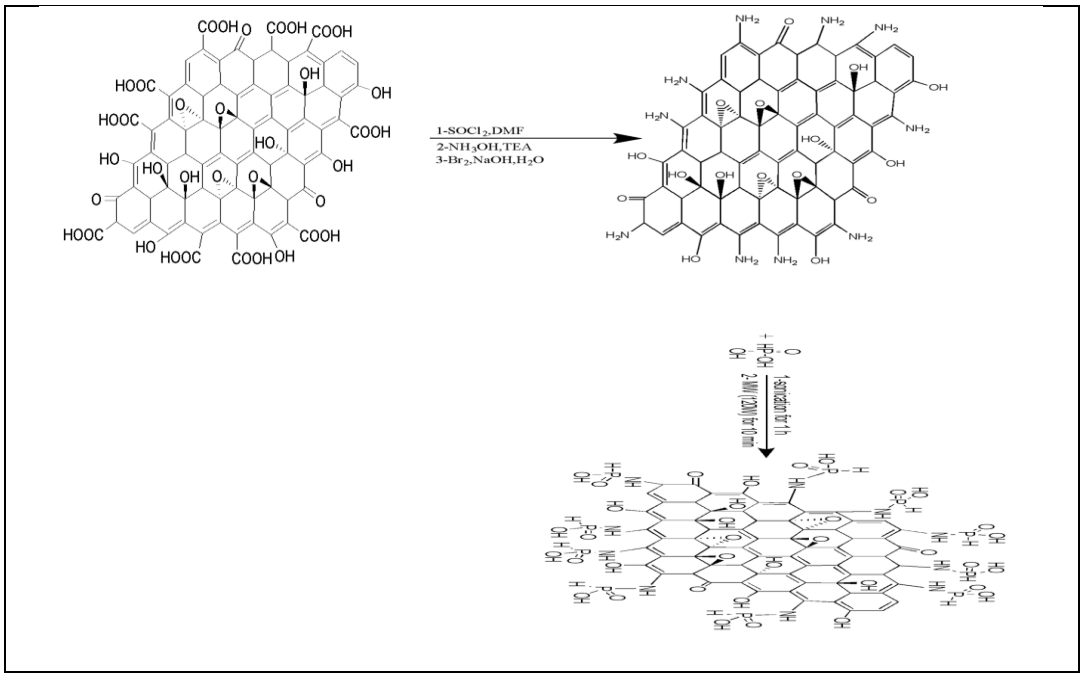

Scheme2: The chemical synthesis of GOE compound.

2.4. Preparation of working electrode for measure Tafel plot and EIS

Pieces of carbon steel combination (C1025) has three measurements (length 2cm),(widths 2.55) and (thicknesses 0.35), the complete area for strips is 12.4925cm2, which inundated in arrangement , then ground with expanding grades Silicon carbide paper for various smoothness (80,120,400,600). A while later they washed with distilled water, ethanol and dried, at that point put away in a dry spot at room temperature 25 C° and set in desiccators which containing silica gel to reason for the shield from the moisture. While in EIS method was used the same methods of cutting, grinding and polishing that applied in corrosion process of the tested metal specimen had been used in EIS impedance. The prepared specimen then washed with distilled water, ethanol and acetone and afterwards stored in a desiccator containing silica gel to keep them away from the moisture

'2.5. The Electrochemical Cells for Tafel plot and EIS

Electrochemical cell of corrosion test that utilized in the present examination, the cell comprises of 100 ml vessel associated with three electrodes were orchestrated as following: Platinum, working and calomel electrode. While EIS method is consist of

10ml cylindrical glass tube and a Teflon cap on the top with two holes to hold a graphite counter electrode and Ag: AgCl reference electrode. The lower part of the cell tube mounted on the coated area of the working electrode.

2.6. Potentiodynamic(Tafel plot) and Impedance spectroscopy (EIS) studies

Potentiodynamic method normally utilized for estimating corrosion resistance and wide assortment of capacities, to gauge current thickness versus electric potential , through set up open circuit potential (OCP) for 20min .The polarization bend can be obtained by checking the potential territory between - 2.5 to +2.5 mV (versus OCP) utilizing a PC for potentiostat/galvanostat at an examining pace of 10 mV S-1. While in EIS method versus Frequency method, it quantifies the impedance spectroscopy of the electrochemical framework in distinction Frequency extend with 100 KHz to 0.01 Hz relating to the open circuit potential (OCP), OCP will show the current of the real open circuit capability of the electrolytic cell after 20 min of inundation in 0.1M HCl (OCP) was refreshed each second.

2.7. Prepare solutions for Potentiodynamic and coating of alloy for EIS method

Potentiodynamic(Tafel plot) the synthesized inhibitors were individually prepared at different concentrations (10, 30, 50, 70 and 100) ppm at 298K with 0.1M HCl as corrosive media. While in this study, EIS method was used to evaluate the adsorption GO and GOE as paint additives to alkyd paint by mixing one of the prepared compounds in different weight percentages with the dye (alkyd resin), these mixtures were used as coat on the surface of carbon steel alloy.

The structure of alkyd paint resin is shown in Figure1. The synthesized inhibitors GO and GOE were added with weight percentages as shown in Table 2 to the alkyd paint and mixed together well in a pitter dish. The standard weight of alkyd resin weight was (0.3g) at 100%.Then in order to prepare the following weight percentages (10%, 15%, 20% and 25% w/w) the amounts of (0.03, 0.045, 0.06 and 0.075g) of each of Go and GOE were added respectively. A small brush was used to coat part of the carbon steel specimen with the mixture of GO or GOE and alkyd paint. The paint thickness was adjusts to (0.2mm) by especially adjusting scrapper in order to distribute the mixture homogenously on the surface of $1cm^2$ of the tested alloy. Coating thickness was measured by a (Vernier) that was sensitive to 0.01mm. A portion of the carbon steel coupon must be exposed (left without coating) in order to make an electrical connection to the working electrode. A portion of the bare metal must be exposed in order to make an electrical connection to the working electrode. The coated carbon steel specimen left to dry for 24 hours.

After the EIS measurements ended the specimen was washed with benzene to remove the paint from the surface of the alloy to be reused again.

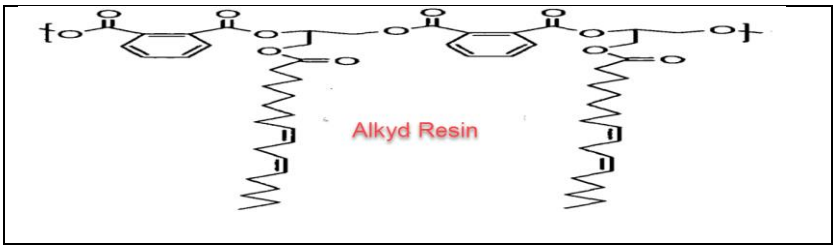

Figure1: The chemical structure of alkyd resin.

Table 2: Weight of inhibitors use as coating in EIS impedance.

NO	Comp	% of inhibitor	Wt. of inhibitor (gm)	Wt. of alkyd resin (gm)
1	GO	10%	0.27	0.03
		15%	0.255	0.045
		20%	0.24	0.06
		25%	0.225	0.075
2	GOE	10%	0.27	0.03
		15%	0.255	0.045
		20%	0.24	0.06
		25%	0.225	0.075

3. Results and discussion

3.1. Characterization by FT-IR spectroscopy of synthesized compounds

The FTIR spectrum of graphene oxide(GO) is shown as the Figure 2 , The broad absorbance band at 3352.39 cm^{-1} is assigned to (OH) stretching vibration, while the strong band at 1728.28 $cm^{-1}$is attributed to Carbonyl group of carboxylic acid(C=O),Furthermore the other bands represents 1585.54, 1408.08,1219.05 and 1045.45$cm^{-1}$are implies to the presence of aromatic ring (C=C), (O-H) bending vibration ,(C–OH)stretching and(C–O–C) epoxy group respectively**[16-19]**.

While the FTIR spectrum of GOE as show in the Figure 3 the sharp band with peak at 3329.25 cm^{-1} is attributed to (OH) vibration stretching for (P–OH), the bands with peaks at 2928.04 and 2850.88 cm^{-1} are attributed to (N-H). The other bands at 1680.22, 1627.97, 1573.97, 1535.39, 1438.94 and 1311.64 cm^{-1} are assigned to for (P–OH) group, aromatic ring (C=C), (N-H) bending vibration, (C–N) stretching vibration, (=CH) bending vibration and (C–OH) stretching respectively.

While the two bands with peaks at, 1242.20 and 895.00 cm^{-1} are attributed to (N–P) due to react with phosphorous acid therefore appeared new bands. The peak at 1087.89 cm^{-1} for (C-O-C) epoxy group, while the two bands at 1049.31 and 806.27 cm-1 are assigned to (P=O). The new absorption peak was appeared at 648.10 cm^{-1}

in the FTIR spectrum of GOE, which was absent in GO through FTIR measurement. Can be attributed to (N–H) out of plan bending vibrations **[8, 14, 20]**.

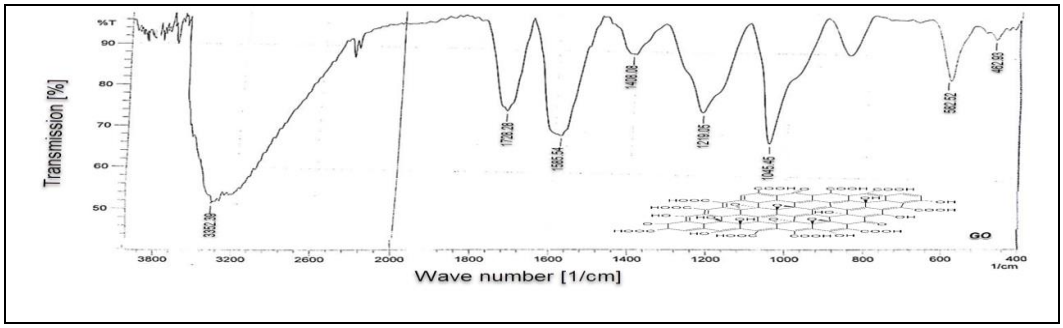

Figure 2: FTIR spectra for GO.

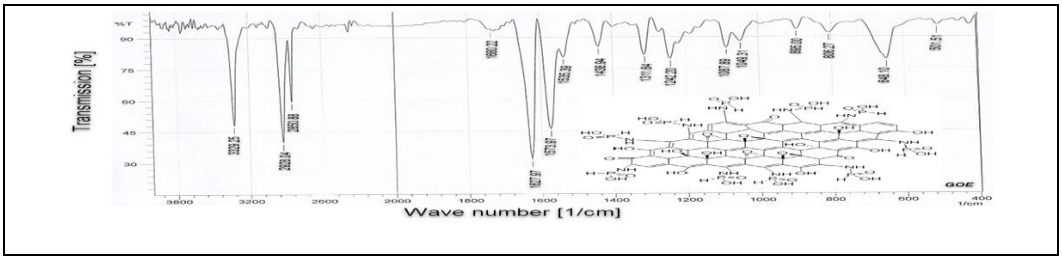

Figure 3: FTIR spectra for GOE.

3.2. Characterization by Raman spectroscopy of synthesized compounds

Raman spectroscopy is wonderful technique for characterization; in the Figure 4 for GO spectra appears there are two clear groups with smal band. first band for D at 1359.57 cm^{-1} that shows to clutter band (confused structures of the sp^2).While second band for G at 1602.48 cm^{-1} that allotted to initially arrange dissipating for in-stage vibration of the E_2g phonon, additionally the vibration method of carbon particles (sp^2), while little band (2D) at 2935.05 cm^{-1} is ascribed to dispersive groups saw in inferred graphite carbon materials**[20]**. While GOE as shown in Figure 5 also appear in two clear peaks at D and G bands small peak for 2D as D band was 1340.35 while the G bands was1602.48 cm^{-1} and another 2D band at 2972.05 cm^{-1} . Raman spectra for GOE it interpreted compared with Raman spectra of GO as starting material. In general D band was blue shifted compared with GO **[20-22]**. This confirms the section of new group on GO surface through functionalization; this is verification of acquaintance some different molecules with carbon layers. While force esteems for GO and GOE noticed that D/G band proportion is a proportion of the turmoil, that uncovers the level of in-plane imperfections and edge deserts in carbon materials, there is change in powers ID/IG proportion on account of electronic conjugation

condition of the GO during adjustment where ID/IG groups proportion of GO and GOE were 0.9 and 0.99 respectively, that implies ID/IG proportion of GO is lower than GOE, where ID/IG estimations of GOE shows to increment in clutter in GO cross section after alteration and demonstrates to diminish in the normal size of the sp2 carbon molecules. This outcome recommending which GO functionalized with phosphorous acid through reaction **[22-25]**

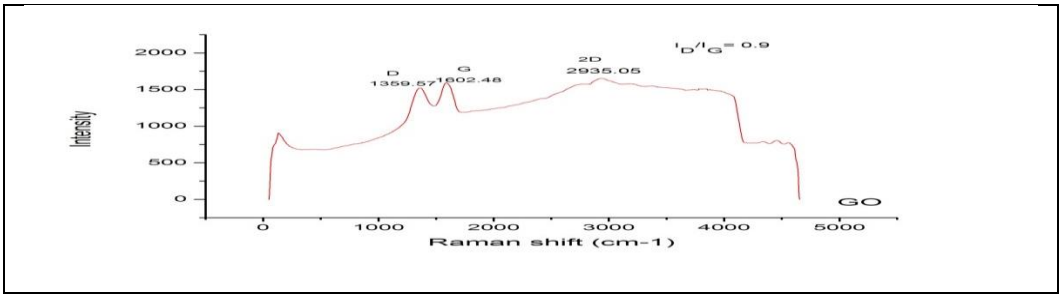

Figure 4: Raman spectra for GO.

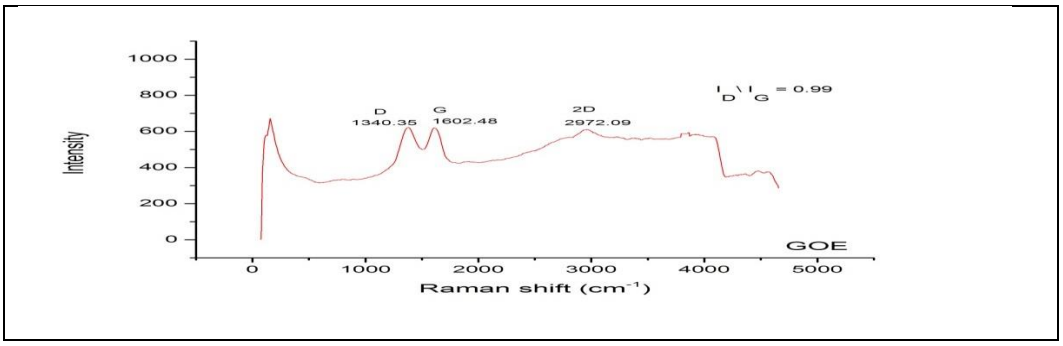

Figure 5: Raman spectra for GOE.

3.3. Characterization morphological surface by FESEM of synthesized compounds

The FESEM image of GO as shown in Figure 6(a) has a flat smooth sheet, kinked areas ,low thickness and a lot of wrinkled edges. The surface of GO is light gray color, consists of several layers, cavities and crumpled flakes**[26]**. While the FESEM image of GOE as shown in Figure6(b) the surface of GOE was flat and consist of sharp edges, some the layers was little, small and light gray color .And also the surface was corrugation and crumpling areas.

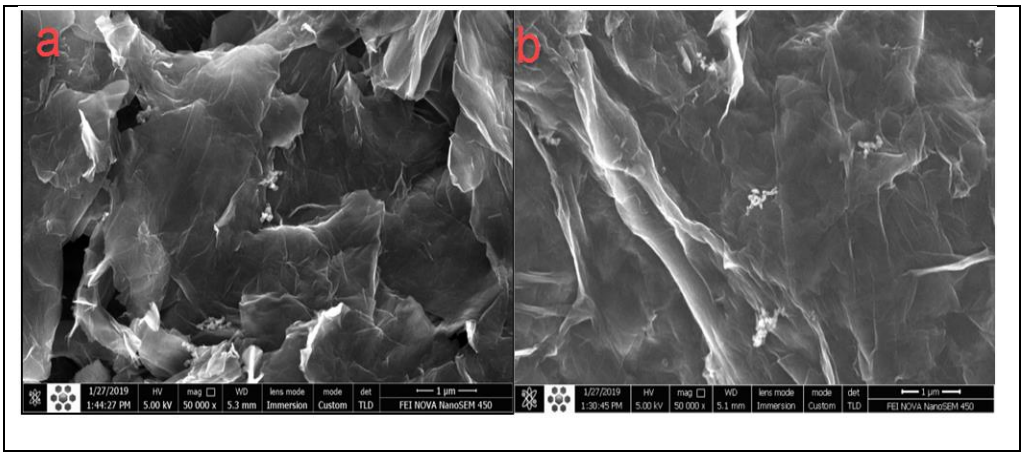

Figure6: FESEM Images for synthesized compounds a: GO and b: GOE.

3.4. Analysis of elemental composition of synthesized compounds by EDS

EDX spectra of GO as shown in the Figure7and Table 3, reveals two peaks assigned to C and O at 0.277 and 0.525 Kev of energy respectively with 71.45 , 28.55 weight% and 76.83 , 23.17 atomic% for C and O and respectively , this indicates that synthesized GO. While EDX spectra of GOE as shown in the below figure 8and Table 4 in this spectra it was that noted there are appear new peaks, at 2 Kev and 0.392 Kev for P and N respectively .and also there is Other element was present as impurities on the surface GOE with new peak at 2.71 Kev is attributed to Cl atom but this peak was present very little in weight and atomic percentage 0.03(Cl) wt% and 0.01(Cl) at%. This evidence suggests successfully of synthesized of GOE in the present study **[23, 27]**.

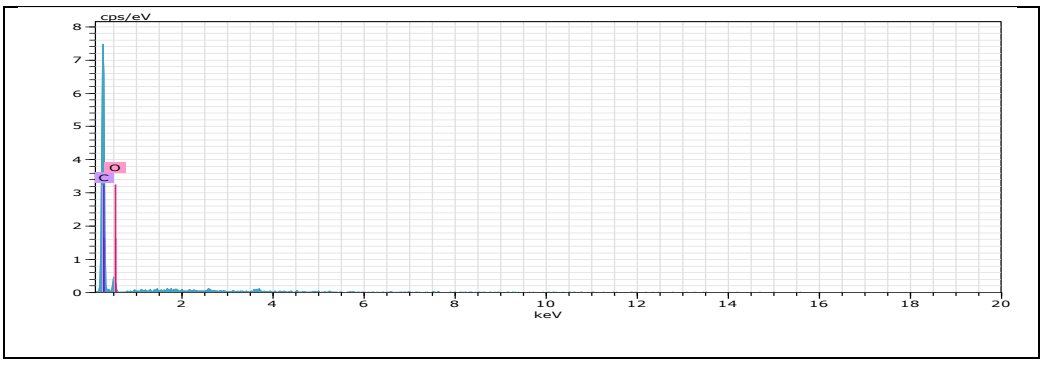

Figure7: EDX spectra of GO.

Table3: EDX spectra analysis for GO.

Element	AN.	Series	Kev	[norm.wt. %]	[norm.at. %]
C	6	K-series	0.277	71.45	76.83
O	8	K-series	0.525	28.55	23.17
Sum:				100	100

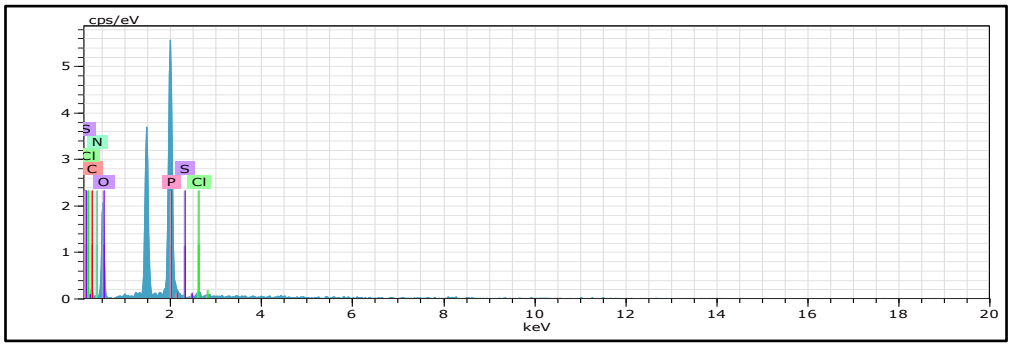

Figure8: EDX spectra of GOE.

Table4: EDX spectra analysis for GO.

Element	AN.	Series	Kev	[norm.wt. %]	[norm.at. %]
C	6	K-series	0.277	38.90	50.41
O	8	K-series	0.525	34.57	33.59
P	15	K-series	2	22.05	11.06
N	7	K-series	0.392	4.45	4.93
Cl	17	K-series	2.71	0.03	0.01
S	16	K-series	2.307	0	0
			Sum:	100	100

3.5. Characterization of synthesized compounds by X-ray Diffraction (XRD)

The XRD spectra of GO as shown in Figure 9 has sharp band at 2θ = 11.15◦ relates (d separating =8 Aº). GO is the result of the oxidation method of graphite powder, as indicated by inquire about distributed internationally affirmed the graphite has reflection (002) top at 26.6° relates (d separating =3.3 Aº). In GO demonstrated that disappearance of band of graphite and new reflection 002 pinnacle showed up at11.15◦ ,where the interlayer dispersing expanded to 8 Aº , because of the nearness of oxygen-rich gatherings containing useful gatherings on the two sides of GO, this affirms the oxidation of graphite into GO effectively. where peak for GO shifted to lower from 11.15◦ to 1.36◦(GOE) after modification of GO the interlayer spacing increased to 65 (GOE) this increase in the interlayer spacing of samples through compared to GO, signifies indicates that new groups attached with the GO surface successfully. From Figure10 shown new peak appeared of GOE compound at 27.47 .that lead to formation disordered stacking structure in functionalization of GO**[9, 19, 25, 28]**.

From XRD data and using Scherrer formula, crystallite size can be calculated for the synthesized of compounds, as in the following equation**[29]**:

$$D = \frac{K\lambda}{\beta cos\theta} \quad \ldots\ldots\ldots\ldots\ldots\ldots\ldots\ldots\ldots\ldots\ldots\ldots\ldots\ldots\ldots \; 1$$

Where D is crystallite size in nm, λ is wavelength of x-ray (0.15406 nm for Cu kα), K is Scherrer constant (0.9) that depends on shape of the crystal, β: is full width half maximum (FWHM) of intensity, θ is Bragg angle.

d-Spacing of XRD patterns for the synthesized compounds by using Bragg's law as in the following equation:

$$\lambda = 2\, d \sin\theta \quad \ldots\ldots\ldots\ldots\ldots\ldots\ldots\ldots\ldots\ldots\ldots\ldots\ldots\ldots\ldots \; 2$$

Whereλ,θ and d were wavelength, Bragg angle and interlayer spacing of crystal respectively. From Table5 reveals that crystallite sizes GO and GOE were7.28 and 0.28 respectively .where noted that crystallite size of GO is higher compared with GOE due to modification of GO.

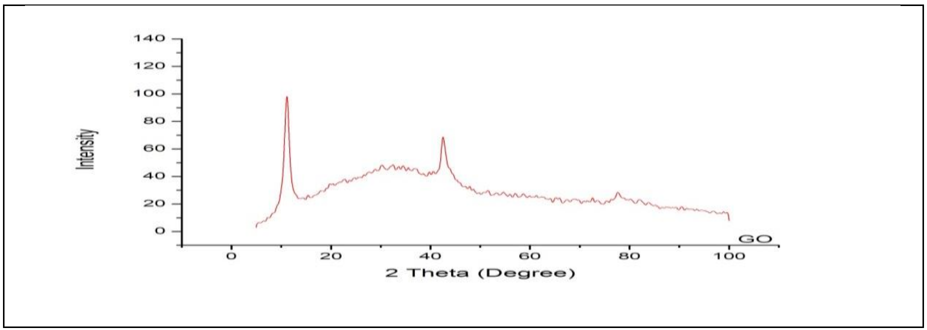

Figure 9: XRD spectra for GO.

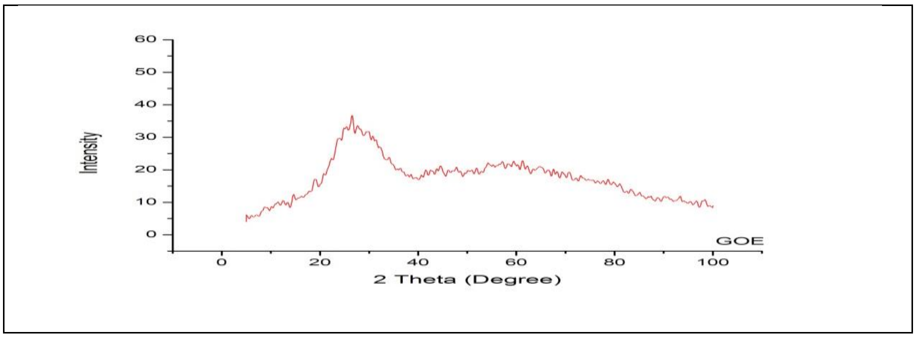

Figure 10: XRD spectra for GOE.

Table 5: parameters for synthesized compounds derived from XRD.

No	Samples	2Theta degree	Distance(d002) (Å)	FWHM degree	Crystallite Size (nm)
1	GO	11.15◦	8	1.097	7.28
2	GOE	1.36◦	65	28.648	0.28

3.6. Polarization studies (Tafel plot)

Concentration effect of the certain inhibitor was studied for synthesized compounds (GO and GOE) at range of 10,30,50,70 and100 ppm at constant temperature 298K by using Tafel plot method .Tafel curves of the above inhibitors are showing as in Figure 11 (a and b). An electrochemical data by using Tafel plots for carbon steel alloy C1025 in presence of corrosive medium (0.1 M of HCl) and presence of both corrosive medium and certain concentration of particular inhibitor were tabulated as in Table 6. This table also shows the other electrochemical factors obtained from the polarization curves including corrosion current density (I_{Corr}), corrosion potential (E_{Corr}), Tafel constants (βa and βc), Polarization resistance (R_p), inhibition efficiency (IE%) and Surface coverage (θ).All of those parameters are affected and are significantly changed by increasing of concentration for above inhibitors.

From Table 6 as concentration of GO increased, its inhibition efficiency was increased from 10 ppm to 100 ppm where CR, I_{corr} are reduced and R_P are increased. This is because of increasing the ability of GO film to protect the surface of alloy C1025 by covering it by thick film that retard the corrosive species as in values in Table 6, where the optimal concentration is 100 ppm. While in case of GOE is may be belong an experimental error, the IE % of GOE is 68.2% at 10 ppm was increased to 86.8% at 70 ppm then reduced to 75.5% this is also because the effect of compatibility . As shown in Tables 6 the corrosion rates decreases significantly with different concentrations of used inhibitors compared to their absence. The corrosion rate of C1025 steel in 0.1M HCl at 298K (the Blank solution) was high (505.54 mpy). By adding GO or GOE to the test solution, these compounds acted as inhibitors by reducing corrosion rates of carbon steel with optimum concentrations of 70ppm for GOE and 100ppm for GO with optimum corrosion rates follows the order: GO (114.24 mpy) > GOE (67.078 mpy) This indicates the effect inhibitors in reducing corrosion rate of carbon steel. The results show that (CR) was decreases with the presence of inhibitor but the relations between the corrosion rate and inhibitors concentration are nonlinear for some compounds. The Potentiodynamic polarization curves (Tafel plots) are those graphs of applied potential versus registered logarithmic current density, Due to that, corrosion current density I_{corr} is estimated by extrapolation of straight part of the measured current. At the intercept point (I_{corr}) the value of corrosion current density is equal for anodic and cathodic reactions, that is, the parameter has a direct influence on the corrosion rate as shown in Figure 11 which represent the Potentiodynamic polarization curves (Tafel plots) for GO and GOE as a function of different inhibitor concentrations at constant temperature.The effects of the inhibitor concentrations on the corrosion current density I_{corr} at 298 K in the presence and absence of inhibitors are listed in Table 6 .The corrosion current of the blank solution of C1025 steel in 0.1M HCl at 298K is (1092 μA/cm^2)**[30]**. The values of I_{corr} with inhibitors are decreased significantly and

almost linearly with the increasing of inhibitors concentrations of (10, 30, 50, 70,100 ppm) respectively. Since the corrosion current is directly proportional to the corrosion rate,therefore, the corrosion currents for GO and GOE are arranged as: GO (246.7 μA/cm^2) > GOE (144.9μA/cm^2 at optimum inhibitor concentration. It is clear that the values of the corrosion current density I_{corr} are significantly reduced in the case of the use of GO and its derivatives as inhibitors compared to the blank solution. The change in current density is due to the formation of a protective layers of inhibitors that adsorbed on the surface of the metal, that leads to introduce a high electrical resistance between the solution and the metal surface and then the change of the current density will leads to changes in corrosion rates**[31, 32]**.

When metals electrodes are immersed in an electrolyte solution, an electrode potential will occurs. After reaching equilibrium, this potential called open circuit potential OCP, which is a difference in potential of microcells of the metal. At that potential, oxidation and reduction reactions occur which allows estimating if the tested metal is resistant to corrosion in tested environment. The higher value of OCP reveals the higher corrosion resistance of the metal. During the Potentiodynamic polarization the potential was shifted from OCP and it called corrosion potential (E_{corr}).Tables 6 show that the values of (E_{corr}) were varied by increasing concentration of all used inhibitors compared to blank. The corrosion potential (E_{corr}) for the blank is - 611mV for blank, while E_{corr} have values of (- 603, and -587 mV) at the optimum concentration of GO and GOE respectively. There are little changes or little displacements between the (E_{corr}) in the presence of inhibitors and blank. The corrosion potential of C1025 steel in 0.1 M HCl at 298K shifted to the slight negative and positive sides (average displacement ≈ (-50mV) - (+24mV) mV) (vs. SCE) relevant to (E_{corr}) of the blank .By depending on the values of (E_{corr}), the compound can be classified as anodic, cathodic or mixed inhibitor. If the value of (E_{corr}) in the presence of the inhibitor is greater than the value of the blank, and this indicates that inhibitor is behaves anodic behavior. In the other way, the inhibitor shows cathodic behavior. Also it can be known through the difference value E_{corr} in presence and absence of inhibitor is lesser than -85 **[5, 6]** this indicates that inhibitor is mixed type. In this study GO and GOE shows a mixed types inhibitors**[32, 33]**.

A Tafel plot, which is a graphical relationship between the current generated in an electrochemical cell and the electrode potential, usually consists of two diverging logarithmic plot lines representing the anodic and cathodic currents. The slop of the straight line tangent to the curve presents Tafel constant values. Tables 6 also presents Tafel constant values that obtained from the polarization curves, represented by the anodic Tafel constant (βa) and cathodic Tafel constant (βc), these constants can explains the behaviors of polarization curves that shown in Figures 11 (a and b) βa and βc values denoted to control in both cathodic and anodic reaction

mechanism, controlled according to βa and βc values in absence and presence of the certain inhibitors. The reaction mechanisms are:

$2Fe \text{ in } C1025 \longrightarrow 2Fe^{2+} + 4e^{-}$ …….... 1

(Oxidation (Anode) dissolution of metal mechanism).

$4H^{+} + O_2 + 4e^{-} \longrightarrow 2H_2O$ ……..……... 2

(Reduction (Cathode) reduction of dissolved O_2 in presence of acid aerated reaction).

Other reaction can be occurred

$2H^{+} + 2e^{-} \longrightarrow H_2$ ……..... 3

(Hydrogen evaluation mechanism (Cathode) reduction).

It may be other reaction can be occurred

$2H_2O + O_2 + 4e^{-} \longrightarrow 4OH^{-}$…… 4

(Reduction of dissolved oxygen).

$$Fe^{+2} + 2OH^{-} \longrightarrow Fe(OH)_2 \xrightarrow{OH^{-}} Fe(OH)_3 \xrightarrow{OH^{-}} 1/2\ Fe_2O_3.3H_2O \quad \ldots\ldots 5$$

The change with addition of inhibitors which suggesting that the inhibitors were first adsorbed on the metal surface and impedes the pass of metal ions from the oxide-free metal surface into the solution, by blocking the reaction sites of the metal surface that affecting both the anodic and cathodic reaction mechanism. The constants results are irregular with the increased in concentration of inhibitors and this means that the synthesized inhibitors were acts as a mixed inhibitors for both cathode and anodic reactions in the corrosive medium**[1, 34]**. The value of I_{corr} can also be estimated by measuring linear polarization resistance which is a quick testing technique for this method the material is polarized. The material's Polarization resistance (Rp) is found by taking the slope of the potential versus current and the corrosion current density is calculated by using Stern-Geary Equation. The Polarization resistance (R_p), results in Table 6 and the Figure11(a and b) showed significantly increasing in (R_p) values with using of the synthesized compounds as corrosion inhibitors on carbon steel in the acidic medium compared with the (R_p) value of the blank ($16.488\Omega.cm^2$)**[30]**.This indicates that the prepared inhibitors can be rise the resistant of the carbon steel surface toward the corrosive acidic medium. At optimum concentrations (100 and 70 ppm) of GO and GOE inhibitors the recorded values of (R_p) are (72.963 and124.26 $\Omega.cm^2$) respectively. Inhibition efficiency (IE %) and Surface coverage (θ) of the metal were calculated from the polarization data in Table 6. These parameters are depending on the value of the corrosion rate, and by increasing the inhibitors concentration there will be subsequence

increases in inhibition efficiencies. At the optimum concentrations of prepared compound the values of the (IE %) are (77.4 and 86.8%) and the values of surface coverage (θ) are (0.774 and 0.868 for GO and GOE at the concentrations of (100and 70 ppm) respectively.

Table6: Corrosion parameters in the absence and presence inhibitors GO and GOE at 298 k.

Comp	Conc (ppm)	Ec_{orr} (mV)	I_{corr} (µA.Cm^{-2})	CR (mpy)	βa mV	βc mV	Rp (Ω.cm^2)	% IE	θ
HCl	Blank	- 611	1092	505.54	214.94	- 240.19	16.488	-	-
GO	10	- 605	412.1	190.82	335.45	- 367.41	43.682	62.3	0.623
	30	- 617	391.5	181.28	214.02	- 394.33	45.982	64.2	0.642
	50	- 605	394.2	182.52	366.64	- 411.11	45.668	63.9	0.639
	70	- 609	309.7	143.41	161.77	- 377.31	58.124	71.7	0.717
	100	- 603	246.7	114.24	443.65	- 458.22	72.963	77.4	0.774
GOE	10	- 618	347.5	160.92	166.28	- 445.31	51.798	68.2	0.682
	30	- 609	290.9	134.69	180.39	- 404.97	40.97	73.4	0.734
	50	- 608	271.3	125.59	257.62	- 554.92	66.369	75.2	0.752
	70	- 587	144.9	67.078	265.19	- 570.49	124.26	86.8	0.868
	100	- 602	267.9	124.02	114.62	- 135.03	67.212	75.5	0.755

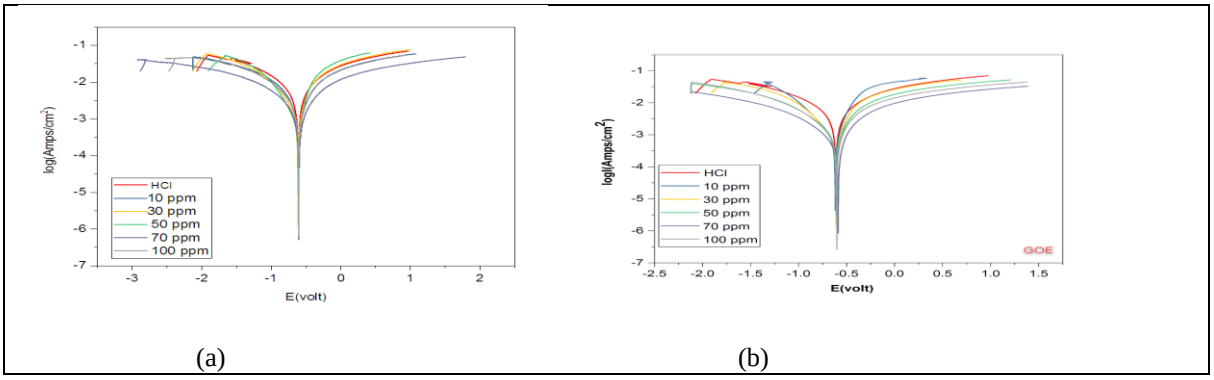

(a) (b)

Figure11: Tafel Plot in the absence and presence inhibitors a: GO and b: GOE at 298 k.

3.7. Impedance Technique (EIS) studies

The impedance system *Z* is a measure of the ability of a circuit to impendent the flow of electrical current. Electrochemical impedance is usually measured by polarizing the electrochemical cell at fixed potential, and then applying an alternating current AC potential (*E*) to perturb the system and measuring the current (*I*) through the cell.

Assume that we apply a sinusoidal potential excitation with small amplitude, and radial frequency ω. The response to this potential is an AC current signal at the same frequency but shifted in phase (*Φ*), the impedance of the *Z* represented as an expression similar to Ohm's law and with Euler's relationship it can be expressed as a complex function**[8]**:

$$Z(\omega) = \frac{E}{I} = Z_0 \exp(j\phi) = Z_0(\cos\phi + j\sin\phi) \quad \ldots\ldots\ldots\ldots\ldots\ldots 3$$

Here, the impedance is therefore expressed in terms of a magnitude Z_o, and a phase shift *Φ*. ***j*** is the imaginary number and ω is the radial frequency (expressed in radians/second) and frequency *f* (expressed in hertz) is:

Here, the impedance is therefore expressed in terms of a magnitude Z_o, and a phase shift *Φ*. ***j*** is the imaginary number and ω is the radial frequency (expressed in radians/second) and frequency *f* (expressed in hertz) is**[35]**:

$$\omega = 2\pi f \quad \ldots\ldots\ldots\ldots\ldots\ldots 4$$

Or $\omega = 2\pi$ F max ……... 5

F max is maximum frequency (Hz).

In order to better analyze the electrochemical impedance EIS characteristics, the data were fitted by the CS Studio 5 software by using *Z*view program to determine the corresponding electrochemical parameters. There are two types of plot obtained from this technique Nyquist and Bode plots for the coated carbon steel alloy in 0.1 M HCl in presence and absence of GO derivatives and alkyd resin mixture as shown in Figures 12-15.

The expression for Z(ω) is composed of a real and an imaginary part. If the real part $\boldsymbol{Z_r}$ (Ω cm^2) is plotted on the X-axis and the imaginary part $\boldsymbol{Z_i}$ (Ω cm^2) is plotted on the Y-axis of a chart, we get a "Nyquist Plot" as in Figures 12 and 13. Notice that in this plot the Y-axis is negative and that each point on the Nyquist Plot is the impedance at one frequency. Nyquist Plot has been annotated to show that low frequency data are on the right side of the plot and higher frequencies data are on the left.

Another plot can be obtained from EIS is the Bode Plot. The impedance is plotted with log frequency F(Hz) on the X-axis and both the absolute values of the impedance ($|Z|=Z_0$) (Ω cm^2) or the phase-shift *Φ* on the Y-axis. The Bode Plot for the coated carbon steel alloy in 0.1 M HCl in presence and absence of GO derivatives and alkyd resin mixture as shown in Figures 14 and 15. Unlike the Nyquist Plot, the Bode Plot does show frequency information.

The EIS data of inhibitors and parameters were calculated and determined by using an electrical equivalent circuit as shown in the Figure 16. There are several parameters appear during fitting of EIS experimental results, all EIS data were listed in Table 7. Such as R_s the solution resistance **[36]** and R_P the polarization resistance

which reflect the protective property, as well as (C_{dl}) which represent the double layer capacitance (μF.cm^{-2}) and was calculated from equation 6: **[36]**

$$C_{dl} = (Y_0 R_p^{1-n})^{1/n} \quad \text{……..…… 6}$$

Where $\boldsymbol{Y_0}$ represents the constant phase element CPE (Ω^{-1} S^n cm^{-2}), the double-layer capacitor ($\boldsymbol{C_{dl}}$) is optimized by using a CPE. $\boldsymbol{R_P}$ the polarization resistance**[36]** (Ω.cm^2) and (***n***) is phase shift of CPE exponent that can be employed as a measure of the roughness of the metal surface. Also ($\boldsymbol{C_{dl}}$) values can be calculated by using the following equation **[36-38]**:

$$\boldsymbol{C_{dl} = \frac{1}{2\pi R_P F_{max}}} \quad \text{……..…. 7}$$

While % IE values can be calculated by using the below equation**[8]**:

$$\%\, \boldsymbol{IE = \frac{Rp(inh) - Rp}{Rp(inh)} \times 100} \quad \text{……..……..…. 8}$$

Where $\boldsymbol{R_{p(inh)}}$ and $\boldsymbol{R_p}$ are polarization resistance magnitudes of mixture GO or its derivatives with dye resin and for the dye resin respectively. While the relaxation time □τ□ □values can be calculated by using the following equation**[39]**:

$$\boldsymbol{\tau = C_{dl} R_P} \quad \text{……..…. 9}$$

A single depressed capacitive loop was observed in the Nyquist plots for GO and GOE as inhibitors when the mixed with dye resin (alkyd), in studied frequency range where the Nyquist loops are depressed semicircles have centers below the real axis. This the depressed semicircle in Nyquist plots was characteristic of solid electrodes which exhibit frequency dispersion because of the morphology of roughness ,surface in homogeneities, surface impurities , inhibitor adsorption and electrode discontinuity. The capacitive loop is associated with electrical double layer (C_{dl}) and charge transfer process. The addition of GO or GOE at different weight percentages does not change the mechanism of corrosion but inhibits corrosion by increasing the (θ) surface coverage with increases of inhibition of efficiency by the adsorbed inhibitor film.

It will noted from Figures 12-15 that the loop diameter of capacitive in presence of GO or GOE with alkyd is larger than with the presence of alkyd resin alone and they increases with increase in weight percentages of inhibitor, this means that radius of semicircles of compounds become large by enhancing inhibitor weight percentage. In the Nyquist spectra, lower frequency are subtracted from higher frequency of real impedance is defining polarization resistance (R_p). Generally, ($\mathbf{R_p}$) includes resistance because of accumulation of corrosion products and inhibitors adsorption at metal/ acid solution interfaces. also it can be notice from the data in Table 6 ,that $\mathbf{R_p}$ values were increased with increased the weight percentages of inhibitors for GO and GOE

that lead to decrease in the corrosion rate **[8, 36, 40-41]**. this suggesting to establishment of protective inhibitor on carbon steel alloy surface , which barrier against charge transfer process .However the adsorption of GO or GOE on corroding surface of carbon steel block of active sites which prone to corrosion .

While C_{dl} and $Y_{\circ}$ values in presence of the inhibitors generally are lower than presence of alkyd only. This change in C_{dl} values lead to formation protective layer on alloy surface, reducing of rate charge transfer process and lead to displacement of water molecules by inhibitors molecules at metal/acid solution interface. This mean that C_{dl} was used to determine the inhibition ability, and indicates that the inhibitors suppressed the corrosion rate of alloy by adsorption mechanism, i.e., decrease the extent dissolution of metals. While ***n*** values (phase shift) if n as a lower value mans that is related to higher roughness surface while if n value was higher it reveals to more homogenous surface i.e., it more smoothness**[8, 40].** In this study from Table 6, n values for GO was increased during the addition of inhibitors compared with alkyd resin, this increasing in n values indicates to increase the smoothness of the surfaces, while ***n*** values of other inhibitors GOE was vary between increase and decrease this mean between smoothness and roughness. On other hand, τ values were increases in most inhibitors this indicates that the adsorbed of inhibitor molecules adsorption on the alloy surface becomes strong that means slow corrosion process. Moreover (% IE) inhibition efficiency was increased as wt.% of inhibitor occurred was increased as in Table 6 **[36]**. The Bode diagrams of GO and GOE as shown in Figures 14-15 that plotted use same experimental data as in the Nyquist plots. In lower frequency range, (Zmod) impedance modulus gives information about corrosion resistance behavior of samples. Where in the figures 14-15 it can be noted that, Zmod values increases with increasing weight percentages of inhibitors compared to dye resin (alkyd) and this reveals that better corrosion inhibition performance of GO and GOE in acidic medium**[41]**.

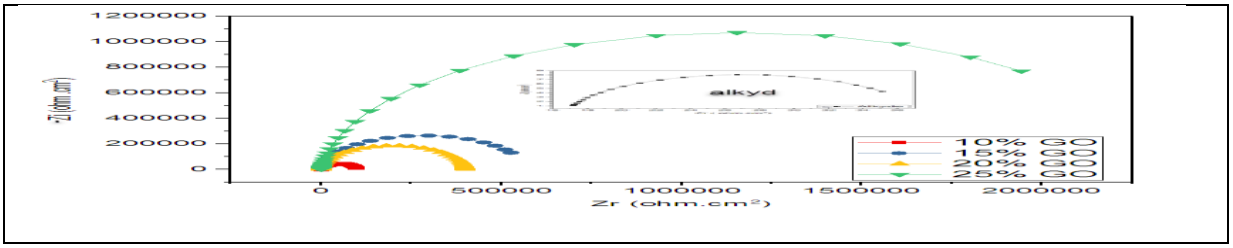

Figure12 : Nyquist diagram for coated C1025 alloy by GO with alkyd resin at 298K.

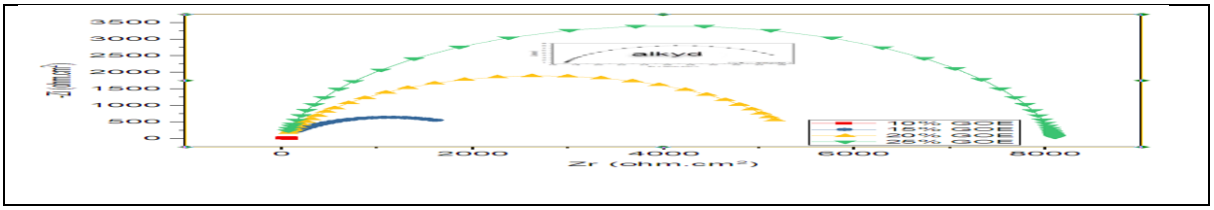

Figure13: Nyquist diagram for coated C1025 alloy by GOE with alkyd resin at 298K.

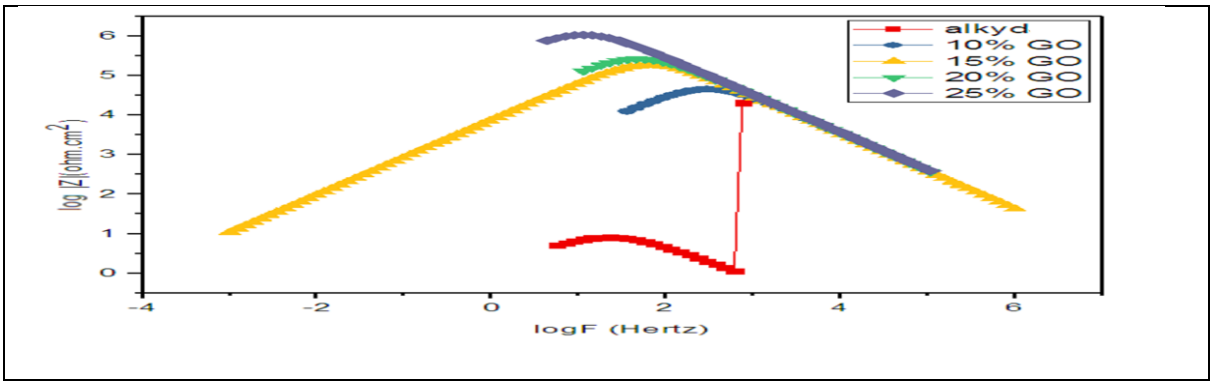

Figure14: Bode plot for a mixture of GO and alkyd resin at 298K.

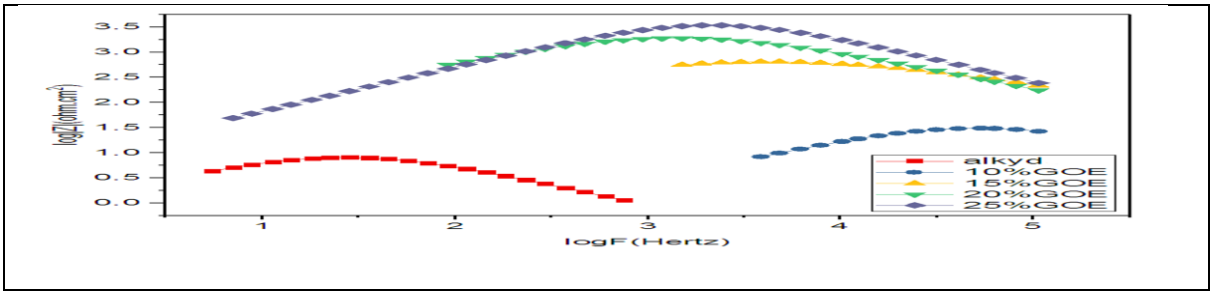

Figure15: Bode plot for a mixture of GOE and alkyd resin at 298K.

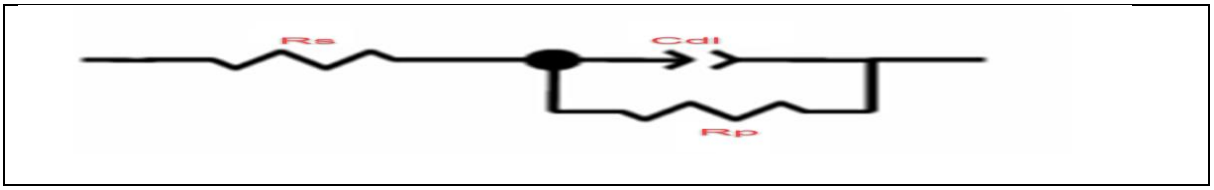

Figure16: An electrical equivalent circuit.

Table 7: Impedance parameters for coated C1025 alloy in presence a mixture of GO and GOE with alkyd resin at 298K.

Inhibit	Wt. % of inhibit	Rp ($K\Omega.cm^2$)	n	Y_o*10^6 ($\Omega^{-1} s^n cm^{-2}$)	Cdl ($\mu F\ cm^{-2}$)	τ *10^3 (s)	Max F (Hertz)	% IE
alkyd	-----	**0.0204**	**0.853**	**613.6**	**282**	**5.8**	**27.008**	----
GO	**10**	**98.571**	**0.947**	**0.0080161**	**0.005392**	**0. 53**	**298.598**	**99.979**
	15	**400.73**	**0.948**	**0.0083574**	**0.00617**	**2.5**	**64.490**	**99.994**
	20	**569.8**	**0.952**	**0.0076724**	**0.00585**	**3.4**	**47.64**	**99.996**
	25	**2322.5**	**0.948**	**0.0076439**	**0.00614**	**15**	**11.173**	**99.999**
GOE	**10**	**0.08009**	**0.833**	**0.32174**	**0.0388**	**0.003**	**51132.17**	**74.53**
	15	**2.3267**	**0.643**	**0.61197**	**0.0161**	**0.0038**	**4251.6**	**99.12**
	20	**5.4467**	**0.774**	**0.16181**	**0.02**	**0. 1**	**1405.94**	**99.63**
	25	**8.0871**	**0.891**	**0.025875**	**0.092**	**0.075**	**2129.3**	**99.75**

4. Conclusions

They are many points concluded dependent on the results acquired.

1. A given data by using Tafel and EIS methods reveals to superimpose between two techniques.
2. Synthesized inhibitors are excellent inhibitors for carbon steel in 0.1 M HCl.
3. As conc. of inhibitor increased, IE% will be increase to reached for an optimal concentration, where 70 ppm for GOE while100ppm for GO
4. Inhibitors behave as mixed inhibitors.
5. Polarization resistance (**R_p)** values were increased with increased the weight percentages of inhibitors GO and GOE that lead to decrease in the corrosion rate.
6. A double layer capacitance (Cdl) values were increased with the increase in weight percentages of inhibitors, this indicates to increase inhibition efficiency.
7. τ values were increases for GO and GOE this indicates that the adsorbed of inhibitor molecules adsorption on the alloy surface becomes strong that means slow corrosion process.

5. References

1.R.T. Loto and C.A. Loto. 2012. **Int. J. Electrochem**. Sci. 7, p 9423 – 9440.

2.Hadi Z. Al-Sawaad. 2015. **International Journal of Advanced Research**. 3, p 343 – 361.

3. E. M. Fayyad M. A. Almaadeed , A. Jones , A. M. Abdullah. 2014. **Int. J. Electrochem.** 9, p, 4989 – 5011.

4.Pruthviraj RD. R. 2016. **J Material Sci Eng** . 5, p. 2169-0022.1000226.

5. Ghazoui, A, Zarrouk, A Bencaht, N, Salghi, R, Assouag, M, El Hezzat, M, Guenbour, A, Hammouti, B.2014. **J. Chem. Pharm, Res**. 6, p 704-712.

6.Faili, N.T. 2015.Chemistry Department ,College of Science , Univeristy of Basrah . **ph.D. Thesis**.

7.Rajeev Kumar Gupta, Manisha Malviya, Chandrabhan Verma, Neeraj K. Gupta and M. A. Quraishi. , 2017. **RSC Advances**. **7**(62), p 39063-39074.

8.Nadeem Baig, D. S. Chauhan, Tawfik A. Saleh and M. A. Quraishi.2019. **New Journal of Chemistry**. 43(5), p 2328-2337.

9.Pankaj Gupta and Rajendra N. Goyal. 2016. **Journal of the Electrochemical Society**. 163(13), p B601- B608.

10.Alireza Ashori , Hossein Rahmani, Reza Bahrami.2015. **Polymer Testing**. 48, p 82-88.

11.Leila Shahriary, Anjali A.Athawale.2014. **Int. J. Renew. Energy Environ. Eng**, 2(01), p 58-63.

12.Chi-Wei Lo, Difeng Zhu and Hongrui Jiang.2011. . **Soft Matter**. **7**(12), p 5604-5609.

13.Chenzhen Zhang, Rui Hao, Hanbin Liao, Yanglong Hou.2013. **Nano Energy**. 2(1), p 88-97.

14.Wenbo Zhang, Jianzhong Ma, Dangge Gao, Yongxiang Zhou, Congmin Li, Jiao Zha, Jing Zhang.2016. **Progress in Organic Coatings**. 94, p 9-17.

15.Ya-Qiong Li , Yun-Bin Chen , Zhi-Zhen Huang .2014. **Chinese Chemical Letters**. 25(12), p 1540-1544.

16.Sanny Verma, Harshal P. Mungse, Neeraj Kumar, Shivani Choudhary, Suman L. Jain, Bir Sain and Om P. Khatri.2011. **Chemical communications**. 47(47), p 12673-12675.

17.ZongxueYu,HaihuiDi,YuMa,YiHe,LingLiang,LiangLv,XiangRan,YangPan,ZhiLuo.2015. **Surface and Coatings Technology**. 276, p 471-478.

18.Jing Wang, Hong-Zhang Geng, Zhi-Jia Luo,a Songting Zhang, Jinqiu Zhang, Juncheng Liu, HaiJie Yang, Sujun Ma, Baoquan Sun, Yan Wang, Shi-Xun Da and Yun-Qiao Fu.2015. **RSC Advances**. 5(127),p 105393-105399.

19.Sumita RANI, Dinesh KUMAR, Mukesh KUMAR.2015. . **Sensors & Transducers**. 193(10), p 100.

20.Kamila Żelechowska, Marta Prześniak-Welenc, Marcin Łapiński, Izabela Kondratowicz and Tadeusz Miruszewski.2017. **Beilstein journal of nanotechnology**. 8(1), p1094-1103.

21.Paulchamy B, Arthi and Lignesh BD.2015. **J Nanomed Nanotechnol**. 6(1), p 1-4.

22.Abhisek Gupta, Bikash Kumar Shaw and Shyamal Kumar Saha. 2014.**RSC Advances**. 4(92), p 50542-50548.

23. Shweta Kumari, Amiya Shekhar, and Devendra D. Pathak.2016. **RSC Advances** 6(19), p 15340-15344.

24.Mohd Hazani Mat Zaid, and Jaafar Abdullah.2017**. in AIP Conference Proceedings** AIP Conf. Proc. 1877, 040002-1–040002-6.

25. BingXue, JiaguiZhu, NaLiu,YongxinLi.2015. **Catalysis** Communications.64, p 105-109.

26. Akhil V Nakhate , and Ganapati D. Yadav.2016. **ACS Sustainable Chemistry & Engineerin**g, 2016. 4(4), p 1963-1973.

27.Himanshu Kharkwal , H.C. Joshi, K.P. Singh.2018. **International Journal of Biochemistry and Biophysics**. 6(1), p 1-19.

28.Yuan-Hsiang Yu, Yan-Yu Lin, Chia-Hsuan Lin, Chih-Chieh Chan and Ying-Chieh Huang.2014. **Polymer Chemistry**. 5(2), p 535-550.

29.Ahmad Monshi , Mohammad Reza Foroughi , Mohammad Reza Monshi.2012. **World journal of nano science and engineering**.2(3), p 154-160.

30.Ali A.Naser, Alaa S. Al-Mubarak and Hadi Z. Al-Sawaad .2019. **Int. J. Corros. Scale Inhib**. 8**,** no. 4, 974–997.

31.A. Ostovari, S.M. Hoseinieh , M. Peikari , S.R. Shadizadeh , S.J. Hashemi.2009. **Corrosion Science**.51(9), p 1935-1949.

32.Hawraa Hameed Radey .2018. chemistry Department ,College of Science , Univeristy of Basrah. **phD Thesis**.

33.M. Manssouri , Y. El Ouadi , M. Znini , J. Costa , A. Bouyanzer, J-M. Desjobert , L. Majidi.2015. **J. Mater. Environ. Sci**. 6(3), p 631-646.

34.H. Serrar , M. Larouj , H.L. Gaz, Z. Benzekri , A. Zarguil , H. Essebaai , S. Boukhris , H. Oudda , R. Salghi , A. Hassikou and A. Souiz.2018. **Portugaliae Electrochimica Acta**.36(1), p 35-52.

35.L. Messaadia ,O. ID El mouden , A. Anejjar , M. Messali , R. Salghi, O. Benali , O. Cherkaoui , A. Lallam.2015. **J. Mater. Environ. Sci**.6, p598-606.

36.Fdil, Rabiaa, Tourabi, M, Derhali, S, Mouzdahir, A, Sraidi, K, Zarrouk, Abdelkader and Bentiss, Fouad.2018. **J. Mater. Environ**. 9, p 358-369.

37.Y. Elkhotfi , I. Forsal , E.M. Rakib and B. Mernari.2018. **Portugaliae Electrochimica Acta**.36(2), p 77-87.

38.Ambrish Singh , Ashish Kumar Singh and M. A. Quraishi.2010. **The Open Electrochemistry Journal**.2(1), p 43-51.

39.Ali Dehghani , Ghasem Bahlakeh , Bahram Ramezanzadeh , Mohammad Ramezanzadeh. 2019. **Journal of the Taiwan Institute of Chemical Engineers**. 102, p 349–377

40.Rajeev Kumar Gupta, Manisha Malviya, Chandrabhan Verma and M.A. Quraishi. 2017.**Materials Chemistry and Physics**. 198, p 360-373.

41.Mudigere Krishnegowda Pavithra, Thimmappa Venkatarangaiah Venkatesha, Mudigere Krishnegowda Punith Kumar, Nanjanagudu Subba Rao Anantha.2015. **Journal of Electrochemical Science and Engineering**.5(3), p 197-208.